

Optimal Coupling Combinations among Discharge Rate, Lateral Depth and Irrigation Frequency for Subsurface Drip-irrigated Triploid *Populus tomentosa* Pulp Plantation

Benye Xi ^{1*}, Ping Wang ^{1*}, Teng Fu ², Weidong Zhang ³, Tan Deng ⁴, Liming Jia ¹

¹ Key Laboratory for Silviculture and Conservation of Ministry of Education, Beijing Forestry University, Beijing 100083, China

² The New School, 66 West 12th Street, New York, NY 10011, USA

³ The Third Affiliated Hospital of Zhengzhou University, Zhengzhou, Henan 450052, China

⁴ Henan Provincial Institute of Forest Inventory and Planning, Zhengzhou, Henan 450045, China

*These authors contributed equally to this work

jjalm2011@yahoo.com.cn

Abstract: This study was conducted to establish the optimal combinations among discharge rate, drip lateral depth, and irrigation frequency for drip-irrigated triploid *Populus tomentosa* pulp plantation through numerical simulation using the HYDRUS (2D/3D) software. Aggregately 18 scenarios of different combinations among three discharge rates (1, 2, and 3 L·h⁻¹), three drip lateral depths (10, 20, and 30 cm), and two irrigation frequencies (continuous irrigation, and pulsed irrigation with water applied intermittently in 30 min periods) were simulated. The results indicate that the RMAE of simulation results at the end of irrigation and approximately 24h later were 7.8 and 6.0% respectively, and the RMSE were 0.0361 and 0.0255 cm³·cm⁻³ respectively, which supports the use of HYDRUS as a tool for investigating and designing drip irrigation management practices. The combination among various discharge rates, frequencies, and drip lateral depths had an obvious effect on the root water uptake, surface evaporation and drainage, with scenario 3C₁₀ and 3C₂₀ had the relative high irrigation efficiency, which were 53.1 and 53.2% respectively. However, from the perspective of increasing irrigation efficiency and reducing the negative effects on the environment, scenario 3C₁₀ is the better irrigation strategy, because scenario 3C₂₀ had higher summation of soil evaporation and deep leakage while 3C₁₀ had more water retained in the active root zone (0-30 cm). In conclusion, the combination of 3 L·h⁻¹ discharge rate, 10 cm lateral depth, and continuous irrigation is the optimal drip irrigation management strategy in the triploid *P. tomentosa* pulp plantations.

[Xi BY, Wang P, Fu T, Zhang WD, Deng T, Jia LM. **Optimal Coupling Combinations among Discharge Rate, Lateral Depth and Irrigation Frequency for Subsurface Drip-irrigated Triploid *Populus tomentosa* Pulp Plantation.** *Life Sci J* 2013; 10(1):3466-3476] (ISSN: 1097-8135). <http://www.lifesciencesite.com>. 438

Keywords: HYDRUS; subsurface drip irrigation; *Populus tomentosa*

1. Introduction

With the rapid development of national economy, the paper industry has become a high-growth industry of production and consumption in China. In 2008, the national production and consumption of paper and paper board were 79.8 and 79.4 million tons respectively, and the consumption will reach 85 million tons in 2010 (**Error! Reference source not found.** PA, 2009). The paper industry in China has a good long-term development potential and social need, but the sustainable development of paper industry meets a serious problem of fibrous raw material supply shortage (**Error! Reference source not found.**, 2008; **Error! Reference source not found.** *et al.*, 2009). In 2008, the total amount of imported paper fiber was 28.9 million tons, accounting for 39% of paper industry raw materials in China (**Error! Reference source not found.**, 2009). The lack of fiber raw materials will not only constrain the healthy development of paper industry in China, but also form highly dependence on foreign resources. The paper industrial safety and competitiveness is under no effective protection

condition. Short-rotation poplar plantations have been identified as a potential source of wood and fiber in China (**Error! Reference source not found.** *et al.*, 2003). Therefore, it is in urgent to develop poplar pulp plantations and promote the forestry-paper integration process. Triploid *Populus tomentosa*, a new clone for short-rotation pulpwood forestry (**Error! Reference source not found.** *et al.*, 1998), plays a key role in fast-growing and high-yielding poplar plantations in the North China Plain. However, due to the lack of technical standards for management, the production of triploid *P. tomentosa* pulp plantation is still very low in general, much lower than its potential productivity. Thus, it is imperative to establish efficient silviculture practices to increase the productivity of these existing *P. tomentosa* plantations.

Controlling genotype, tree density and nutrient availability are the traditional methods to increase the plantation productivities (**Error! Reference source not found.** *et al.*, 2004; **Error! Reference source not found.** and Hartsough, 2006; **Error! Reference source not**

found. *et al.*, 2007). Recently, more and more researchers began to further enhance production by strengthening water and fertilizer management (**Error! Reference source not found.** *et al.*, 2002; **Error! Reference source not found.** and Coleman, 2005; **Error! Reference source not found.** *et al.*, 2005). In china, the main irrigation techniques used in fast-growing and high-yield plantations were flood and den irrigation at present (**Error! Reference source not found.** *et al.*, 2000; **Error! Reference source not found.** *et al.*, 2006). However, due to the severe water scarcity (**Error! Reference source not found.** *et al.*, 2000), it is not allowable to apply a lot of water in forest plantation without restraint. Thus, in the context of sustainable water resources use, increasing the production of plantation by strengthening the water management must adopt water-saving irrigation technology. Micro-irrigation, especially the subsurface drip irrigation (SDI), is a high efficient irrigation method, which can increase productivity while saving water, and has been widely applied in culturing the plantations in the world (**Error! Reference source not found.** *et al.*, 2002; **Error! Reference source not found.** *et al.*, 2005; **Error! Reference source not found.** *et al.*, 2009).

SDI is the most advanced method of irrigation, which can apply small amounts of water directly to the root zone and minimize evaporative losses and deep percolation. Due to its high water use efficiency and environmental sound effect, interest in using SDI to irrigate plantation is growing in China. Consequently, a lot of studies in plantations under SDI have been conducted, and these researches mainly focused on studying the effect of SDI on plantation yield (**Error! Reference source not found.** *et al.*, 2004; **Error! Reference source not found.** *et al.*, 2005), tree photosynthesis (**Error! Reference source not found.** *et al.*, 2004), characteristics of root growth (**Error! Reference source not found.** *et al.*, 2008), etc. or establishing proper irrigation scheduling (**Error! Reference source not found.** *et al.*, 2003). However, specific studies on selecting the optimal SDI system design parameters (such as discharge rate, lateral depth, etc) and irrigation management strategies have not attracted the attention of forestry researchers so far. In fact, improperly performed SDI system may not only necessarily assist plants to function properly and achieve increased production as expected (**Error! Reference source not found.** and Midmore, 2005), but also may have unwanted negative effects on the environment such as ground water pollution (**Error! Reference source not found.** *et al.*, 2009). Therefore, appropriate design and efficient management of SDI is the prerequisite to successfully applying SDI to the cultivation of poplar plantations.

The knowledge on optimal SDI system design parameters and irrigation strategies can be obtained by conducting field experiments. Although this method is direct and accurate, it is limited by laborious, time-consuming, and expensive works. Recently, designing and managing SDI system through numerical modeling of water distribution under SDI has attracted the attention of researchers (**Error! Reference source not found.** *et al.*, 2003; **Error! Reference source not found.** *et al.*, 2006; **Error! Reference source not found.** and Diamantopoulos, 2009). Among these numerical models, HYDRUS is the most widely used model, and has been proved to be an efficient tool in investigating the optimal drip management practices (Cote *et al.*, 2003; **Error! Reference source not found.** *et al.*, 2004; **Error! Reference source not found.** *et al.*, 2005; **Error! Reference source not found.** and Skaggs, 2009). Therefore, the HYDRUS (2D/3D) software was used for the current study. The objectives of this study were (1) to investigate the effects of lateral depth, dripper discharge rate, and irrigation frequency on wetting patterns under the experimental soil through numerical simulation; and (2) to investigate the optimal irrigation strategy for a *P. tomentosa* plantation in the North China Plain

2. Materials and methods

2.1 Field experiment

2.1.1 Experimental site

The experiment was carried out in a triploid *P. tomentosa* pulp plantation of Quan Lin Company (36°58'N, 116°14'E and 27 m above sea level), in Gaotang County, Shandong Province, China (Figure 1). The site possesses a warm temperate monsoon climate with mean annual temperature of 13.2°C, mean annual precipitation of 545mm and mean annual free surface evaporation of 1880mm. The ground water table is about 3m below the ground surface. The region has a typical layered soil, developed from the quaternary alluvium of Yellow River, consisting of about 30cm of sandy loam underlain by about 30cm of loam with another sandy loam beyond about 60cm. Physical properties of the soil are provided in Table 1.

The *P. tomentosa* plantations at the experiment site were established in 2005 with wide and narrow row planting scheme. The wide row spacing is 6 m, narrow row spacing is 2 m and intra-row spacing is 1 m. SDI was applied in the plantation. Drip laterals were placed in the middle of the narrow rows, with a discharge rate of 2 L h⁻¹ and approximately 20 cm installation depths.

2.1.2 Experimental design and measurements

The spatial distribution of *P. tomentosa* fine roots was measured on November 2008. Soil cores (301 cm³) were taken in wide and narrow row respectively, and the sample grid was shown in Figure

2. Soil samples were taken at 20 cm intervals in the vertical direction, and the maximum sampling depth was empirically set as 80cm. In total, 816 soil cores were taken to measure root length density. Roots were washed from the core samples using fresh water. Total root length of the fine roots (diameter < 2 mm (**Error! Reference source not found.** *et al.*, 2006)) was

determined using an automatic image analysis system WinRhizo (Regent Instruments, Inc., Canada). The root length density ($\text{cm}\cdot\text{cm}^{-3}$) of each sample was determined by dividing the total root length by the soil core volume.

Table 1. Soil physical properties at the experimental site

| Soil depth (cm) | Sand (%) | Silt (%) | Clay (%) | Texture ^a | Bulk density ($\text{g}\cdot\text{cm}^{-3}$) | θ_s ^b ($\text{cm}^3\cdot\text{cm}^{-3}$) | θ_f ^c ($\text{cm}^3\cdot\text{cm}^{-3}$) |
|-----------------|----------|----------|----------|----------------------|--|--|--|
| 0-30 | 69.65 | 25.90 | 4.45 | Sandy loam | 1.65 | 0.38 | 0.29 |
| 30-60 | 50.30 | 40.20 | 9.50 | Loam | 1.66 | 0.40 | 0.36 |
| 60-100 | 58.65 | 37.35 | 4.00 | Sandy loam | 1.51 | 0.48 | 0.39 |

^a USDA classification; ^b Saturated soil water content; ^c Field capacity

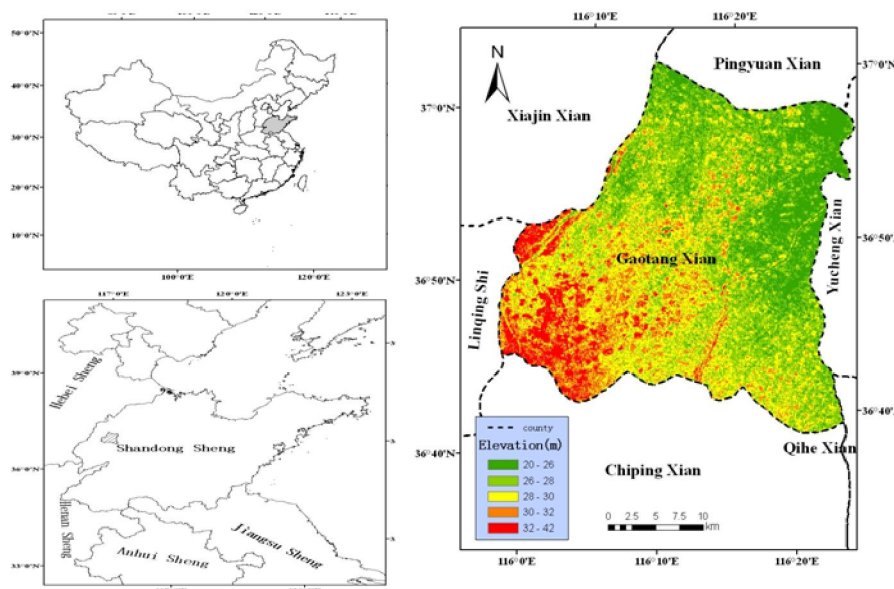


Figure 1. Location of the experimental site

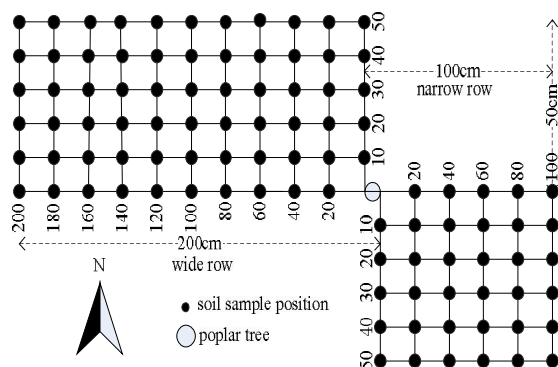


Figure 2. Schematic diagram of soil sample position

2.2 Mathematical model

The infiltration of soil water under SDI is a three-dimensional process in nature. However, in the field it is possible to ignore individual emitters and conceptualize the drip tubing as a line source with infiltration and redistribution being a two-dimensional process (**Error! Reference source not found.** *et al.*, 2004). Thus in our study the drip irrigation was simulated assuming the drip irrigation system can be represented as an infinite line source.

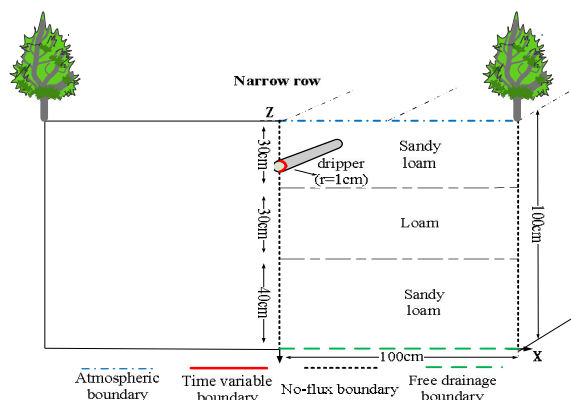


Figure 3. Schematic diagram of simulation area

The HYDRUS (2D/3D) software package (**Error! Reference source not found.** *et al.*, 2006) was used to simulate root zone dynamics of soil water under SDI for *P. tomentosa*. Assuming a homogeneous and isotropic soil and ignoring the influence of air and temperature on water movement, water flow in the root zone was modeled using the following equation which was based on the Richards equation and a macroscopic sink term representing root water uptake.

$$\frac{\partial \theta}{\partial t} = \frac{\partial}{\partial r} \left[\frac{K(h) \partial h}{\partial r} \right] + \frac{\partial}{\partial z} \left[\frac{K(h) \partial h}{\partial z} \right] - \frac{\partial K(h)}{\partial z} - S(z, t)$$

where θ is the volumetric water content ($\text{cm}^3 \cdot \text{cm}^{-3}$), h is the soil water pressure head (cm), z is the vertical coordinate (cm) and assuming that it is positive downward, r is the radial coordinate (cm), t is the time (h), $K(h)$ is the unsaturated hydraulic conductivity ($\text{cm} \cdot \text{h}^{-1}$), $S(z, t)$ is the root water uptake term ($\text{L} \cdot \text{h}^{-1}$). The soil hydraulic properties were specified according to the van Genuchten (**Error! Reference source not found.** Genuchten, 1980) model.

$$\theta(h) = \begin{cases} \theta_r + \frac{\theta_s - \theta_r}{(1 + |\alpha h|^n)^m} & h < 0 \\ \theta_s & h \geq 0 \end{cases}$$

$$K(h) = K_s S_e^l \left[1 - (1 - S_e^{1/m})^m \right]^2$$

Where $\theta(h)$ is the soil water retention ($\text{cm}^3 \cdot \text{cm}^{-3}$); θ_r is the residual water contents ($\text{cm}^3 \cdot \text{cm}^{-3}$); θ_s is the saturated water content ($\text{cm}^3 \cdot \text{cm}^{-3}$); K_s is the saturated hydraulic conductivity ($\text{cm} \cdot \text{h}^{-1}$); S_e is the degree of saturation ($S_e = (\theta - \theta_r) / (\theta_s - \theta_r)$); α , n and l are

Table 2. Predicted soil hydraulic parameters

| Soil depth (cm) | θ_r ($\text{cm}^3 \cdot \text{cm}^{-3}$) | θ_s ($\text{cm}^3 \cdot \text{cm}^{-3}$) | α (cm^{-1}) | n | K_s ($\text{cm} \cdot \text{h}^{-1}$) | l |
|-----------------|---|---|-------------------------------|--------|---|-----|
| 0-30 | 0.0321 | 0.3800 | 0.0502 | 1.4486 | 1.5771 | 0.5 |
| 30-60 | 0.0343 | 0.4000 | 0.0255 | 1.3498 | 0.5967 | 0.5 |
| 60-100 | 0.0302 | 0.4800 | 0.0303 | 1.4137 | 1.9038 | 0.5 |

2.2.4 Root water uptake

Statistical analysis results showed that there

the shape parameters with $m=1-1/n$.

2.2.1 Simulation area

Because the drip line was placed in the middle of the narrow row, thus the rectangular plane perpendicularly to the drip lateral was divided into two symmetrical parts assuming soil water movement will be symmetrical on either side of the drip lateral in course of time and we only simulated the right section of the presumed symmetric profile. The schematic diagram of the simulation area was shown in Figure 3.

2.2.2 Initial and boundary conditions

Observed soil water content in the experimental field was taken as initial condition for water. The boundary condition of the drip tubing, which was represented as a half-circle ($r=1$ cm) on the left boundary was taken as time variable boundary and the remaining portion of the left boundary was set as a zero flux condition due to the symmetry of the profile. The upper boundary was defined as an atmospheric boundary to take the root water uptake and soil evaporation into account while the bottom boundary was specified as a free drainage boundary. The right boundary which is far away from drip tubing was a no-flux boundary.

2.2.3 Hydraulic parameters

Running HYDRUS requires specifying the soil hydraulic parameters θ_r , θ_s , K_s , n , α , and l . The hydraulic parameters were determined with the ROSETTA pedotransfer function model (**Error! Reference source not found.**, *et al.*, 2001) which was included in HYDRUS. Based on the data for the bulk density and percentages of sand, silt and clay that were shown in Table 1, we obtained the estimated parameters that were given in Table 2. In most situations, ROSETTA will provide estimates for θ_r , n , α , and l that are sufficiently accurate for drip irrigation simulation (**Error! Reference source not found.** *et al.*, 2004). However, in order to get more detailed characterization of the soil hydraulic properties, we measured θ_s for different soil layers using Wilcox method (**Error! Reference source not found.**

were no significant differences among the RLD for various radial distance in every soil layer, thus we

concluded that in the narrow row the roots were distributed uniformly and a one-dimensional root water uptake model was suitable to simulate the uptake of water by poplar roots. The one-dimensional root water uptake model can be expressed as:

$$S(z, t) = \alpha [h(z, t)] b(z) T_p(t)$$

Where $S(z, t)$ is the actual root water uptake rate ($l \cdot h^{-1}$); $b(z)$ is the relative root length density distribution function; T_p is the potential transpiration rate ($cm \cdot h^{-1}$); $\alpha(h)$ is the dimensionless soil water stress function that reduces root water uptake due to soil water stress and is given by (**Error! Reference source not found.** *et al.*, 1978):

$$\alpha(h) = \begin{cases} (h_0 - h) / (h_0 - h_1) & h_1 < h \leq h_0 \\ 1 & h_2 \leq h \leq h_1 \\ (h - h_3) / (h_2 - h_3) & h_3 < h < h_2 \\ 0 & h \leq h_3 \end{cases}$$

Where h is the soil water pressure head (cm); h_0 , h_1 , h_2 , h_3 are parameters.

The data for the *P. tomentosa* root distribution indicated that 49% of the total RLD was located in the top 20 cm soil layer, 19% was located between 20 and 40 cm, 12% between 40-60 cm and 20% between 60 and 80 cm. Consistent with this data, we model the root distribution with the following normalized function:

$$b(z) = \begin{cases} 0.0037 / RD & 0 \leq z \leq 20cm \\ 0.00145 / RD & 20 \leq z \leq 40cm \\ 0.0005 / RD & 40 \leq z \leq 60cm \\ 0.0015 / RD & 60 \leq z \leq 80cm \end{cases}$$

Where $z=0$ cm is the soil surface; $z=80$ cm is the maximum rooting depth; $RD=0.152 \text{ cm} \cdot \text{cm}^{-3}$ is the total roots length density.

2.3 Simulation of different irrigation scenarios

A total of 18 irrigation scenarios (Table 3.3) for three different dripper discharge rates ($q=1, 2, \text{ and } 3 \text{ l/h}$), three lateral installation depths ($d=10, 20, \text{ and } 30 \text{ cm}$), and two irrigation frequencies (continuous irrigation, and pulsed irrigation with water applied intermittently in 30 min periods) were examined to evaluate what can be achieved by using different irrigation strategies. Among the 18 irrigation scenarios, scenario 2C₂₀ represents the typical SDI strategy in the cultivation of local poplar plantations, and the other 17 irrigation scenarios are alternative irrigation strategies.

Table 3. Details of irrigation scenarios

| Scenario Code | Discharge rate (L/h ⁻¹) | Lateral depth (cm) | Irrigation frequency |
|------------------|-------------------------------------|--------------------|----------------------|
| 1P ₁₀ | 1 | 10 | Pulsed |
| 2P ₁₀ | 2 | 10 | Pulsed |
| 3P ₁₀ | 3 | 10 | Pulsed |
| 1C ₁₀ | 1 | 10 | Continuous |

| | | | |
|------------------|---|----|------------|
| 2C ₁₀ | 2 | 10 | Continuous |
| 3C ₁₀ | 3 | 10 | Continuous |
| 1P ₂₀ | 1 | 20 | Pulsed |
| 2P ₂₀ | 2 | 20 | Pulsed |
| 3P ₂₀ | 3 | 20 | Pulsed |
| 1C ₂₀ | 1 | 20 | Continuous |
| 2C ₂₀ | 2 | 20 | Continuous |
| 3C ₂₀ | 3 | 20 | Continuous |
| 1P ₃₀ | 1 | 30 | Pulsed |
| 2P ₃₀ | 2 | 30 | Pulsed |
| 3P ₃₀ | 3 | 30 | Pulsed |
| 1C ₃₀ | 1 | 30 | Continuous |
| 2C ₃₀ | 2 | 30 | Continuous |
| 3C ₃₀ | 3 | 30 | Continuous |

In order to be similar to the actual irrigation situation of our experimental site in autumn, the initial water content for 30-60 and 60-100 cm soil layer were specified as 0.23 and 0.18 cm^3/cm^3 respectively, which were the lowest values monitored by the soil moisture sensors. As to the 0-30 cm soil, where most fine roots located, we specified its initial condition as 0.14 cm^3/cm^3 , which equals to -255 cm pressure head in this zone, because in medium-texture soil -200 to -600 cm is the average field soil water tension prior to irrigation (**Error! Reference source not found.** *et al.*, 2005). The root distribution was modeled with Eqs. (7), whereas the parameters h_0, h_1, h_2, h_3 of Eqs. (6) were set to 0, -60, -240, and -10000 cm, respectively. Besides, for simplicity, and because we have no corresponding model to calculate the potential evapotranspiration (ET_p) of *P. tomentosa*, we use the average evaporation and transpiration rate of 20 days, which were monitored just 1 to 3 days after rain or irrigation, as the potential evaporation (E_p) and transpiration (T_p). In our experiment site, the evaporation and transpiration were measured by micro-lysimeter (**Error! Reference source not found.** and Robertson, 1982) and TDP-30, respectively. Simulations for all irrigation scenarios were conducted during a 32 days period (irrigation interval is 4 day), and the applied water amounts equal to 100% of the potential daily evapotranspiration rate ($ET_p = E_p + T_p = 4.5 \text{ mm} \cdot \text{d}^{-1}$).

3. Results and discussions

3.1 Effects of various parameters on the wetting pattern

The geometry of the soil wetted zone is affected by different parameters, including the discharge rate, the lateral depth, the irrigation frequency, etc. Thus numerical simulations were executed to determine the effects of different parameters (Table 3.3) on the geometry of the wetting patterns for the experimental layered soil. In this section, to save space, we only use the selected data of the first irrigation interval.

3.1.1 Emitter discharge rate

Figure 4(a), (b), and (c) showed the influence of emitter discharge rate on the predicted soil wetting patterns (Table 3.3, scenario 1C₂₀, 2C₂₀, 3C₂₀). The corresponding irrigation duration varied according to discharge rate. As the discharge rate decreased, the wetted radius and depth increased. The wetted radius and depth were about 27 and 53 cm for q=3 L·h⁻¹, 28 and 56 cm for q=2L·h⁻¹, and 30 and 56 cm for q=1 L·h⁻¹, respectively. This may be attributed to the limitation of the soil infiltration rate. The dripper with higher discharge rate delivered the total amount of irrigation water in a shorter time and could not spread rapidly to the surrounding soil. On the contrary, the lower discharge rate allowed a larger time to deliver and distribute the same amount of water, subsequently resulting in a greater wetting volume. These observed trends were similar to the results observed for the

uniform soils (Cote *et al.*, 2003). From Figure 4(a), (b),and (c), it can also be seen that the gradients of water content behind the wetting front increased as the discharge rate increased, with much sharper gradients at higher discharge rate, which might also result from the soil infiltration rate limitation. Besides, it can be found that water spread horizontally farther in 30-60 cm than in 0-30 cm, which might be attributed to the hindering effect of the interface between soil layers. Because the penetrability of the 30-60 cm soil layer (loam) was lower than that of the 0-30 cm soil layer (sandy loam), thus when the water wetting front reaches the interface at about 30 cm, the vertical infiltration rate slowed down and more water accumulated beneath the interface, consequently accelerating the horizontal spreading of water.

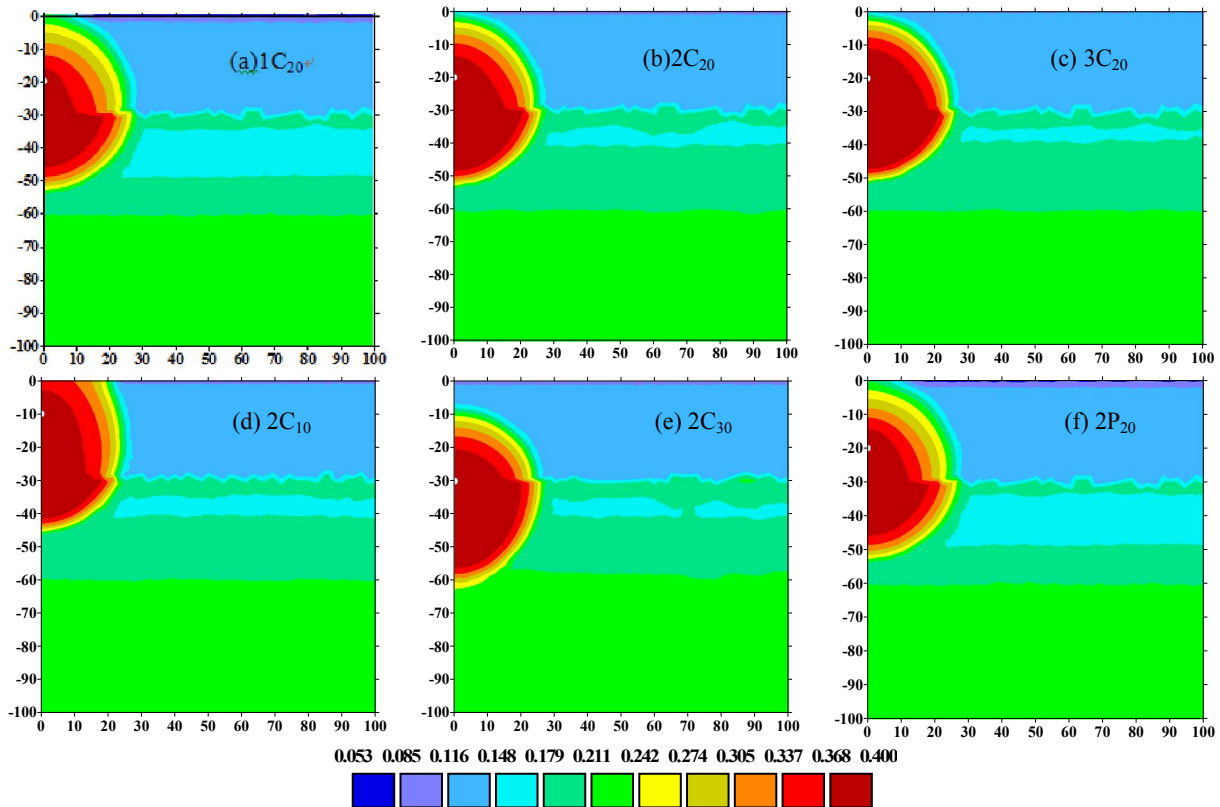


Figure 4. Predicted wetting patterns at the end of irrigation in the first irrigation interval for various combinations of discharge rate, lateral depth, and irrigation frequency (irrigation scenarios selected from Table 3.3).

3.1.2 Depth of drip lateral

The effects of lateral installation depths on the geometry of the wetted zone (Table 3.3, scenario 2C₁₀, 2C₂₀, 2C₃₀) were shown in Figure 4(d), (b),and (e). The wetted volume changed from elliptical to roughly spherical as the installation increased from 10 to 30 cm. The wetted depth increased with the installation depth, which agreed well with the results obtained by Singh *et*

al. (**Error! Reference source not found.**). And the wetted depth was 47, 56, and 62 cm for *d*=10, 20, and 30 cm, respectively. As expected, the wetted radius increased with installation depth as well, which was 24, 28 and 28.5 cm for *d*=10, 20 and 30 cm, respectively. This contradicted the observations of Siyal *et al.* (**Error! Reference source not found.**). This discrepancy might be due to the difference in soil texture and structure.

Furthermore, from Figure 4(d), (b), and (e) it can also be observed that $d=10$ cm allowed the wetting front to spread widely along the soil surface at the end of irrigation, which did not occur in the scenarios of $d=20$ and 30 cm, and the corresponding wetted soil surface area was 22 cm.

3.1.3 Irrigation frequency

Figure 4(b) and (f) exhibited the effect of irrigation frequency on the geometry of the wetting patterns (Table 3., scenario $2C_{20}$ and $2P_{20}$). Pulsed irrigation slightly increased the radius and depth of the wetted volume. Besides, the water content gradient behind the wetting front in pulsed irrigation was less than that in continuous irrigation. These results may be attributed to that pulsed irrigation decreased the average discharge rate from 2 to 1 $L \cdot h^{-1}$ and water redistributed between pulsed water applications, thereby resulting in a slight increase in wetting pattern.

3.2 Water balance and the optimal irrigation strategy

3.2.1 Water balance

The data for the *P. tomentosa* root distribution indicated that more than 50% of the total fine roots were located in the top $0-30$ cm soil layer, therefore we mainly focus on the water storage in this layer at the end of irrigation. Figure 55 showed the final relative water masses for $0-30$ and $30-100$ cm under different

simulation scenarios (Table 3.3). It was clear that, in the $0-30$ cm, the water mass decreased with time because of root water uptake, evaporation and downward percolation (Figure 55). As expected, for given irrigation frequency and discharge rate, the decrease was the lowest for $d=10$ cm due to shallower lateral depth having smaller wetting depth (Figure 4 (d), (b), (e)). For given discharge rate and lateral depth, the lowest decrease occurred in pulsed irrigation scenarios due to pulsed application resulting in farther forward and lateral water transport (Figure 4(b), (f)). When investigated the effect of discharge rate on final water mass, we found that under continuous irrigation $q=1$ $L \cdot h^{-1}$ retained the most moisture for $d=10$ and 20 cm, while $q=3$ $L \cdot h^{-1}$ retained the most moisture for $d=30$ cm. However, under pulsed condition, $q=1$ L/h always conserved the most water regardless of the lateral depth. As to the $30-100$ cm soil layer, different from the trend obtained in the $0-30$ cm, the water mass increased with time, which reflected that in this zone the summation of leaching and root water uptake rate was lower than the inflow rate. In addition, it can be noted that, no matter in continuous or pulsed irrigation, $q=1$ $L \cdot h^{-1}$ had the highest water mass increase for various later depths, but the difference was slight.

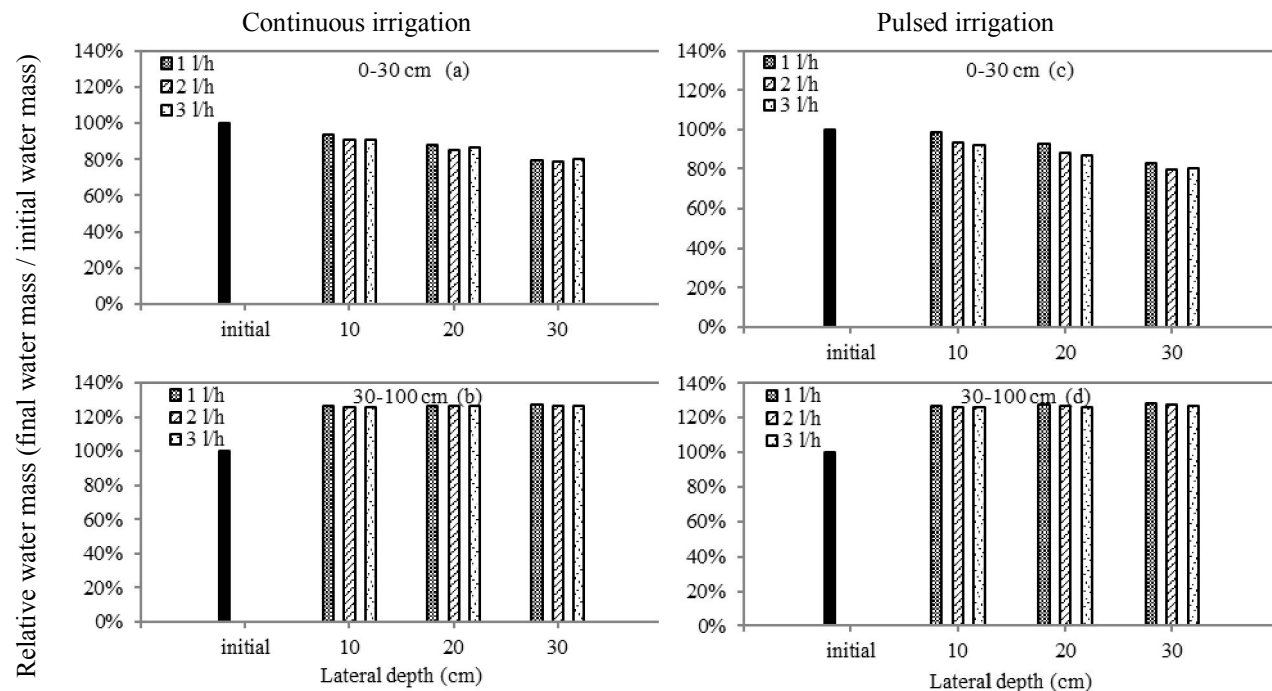


Figure 5. The initial and final relative water masses for (a, c) $0-30$ cm and (b, d) $30-100$ cm soil layer. Values are expressed as a fraction of the initial water mass.

The effects of lateral depth (Table 3.3, scenario $2C_{10}$, $2C_{20}$, $2C_{30}$) and discharge rate (Table 3.3, scenario $1P_{30}$, $2P_{30}$, $3P_{30}$) on the root water uptake were

showed in Figure 6. In all the simulation scenarios, a trend of decreasing occurred for the first 300 h, but thereafter, little trend was found. This may resulted

from that, during the first 300 h, the most active root zone (0-30 cm) had relative sufficient water so that all the roots distributed within this layer absorbed water to their maximum ability. However, the water resource in the root zone where the irrigation water did not reach decreased rapidly with time although the other root zone could be recharged by irrigation, thereby resulting in the overall decline of water uptake with time. In the rest of the simulation period, because of increasing water stress effect, roots hardly absorb water from the difficult recharge water area and most of the water uptake activities occurred within the irrigation wetting volume, which consequently leading to the stable variation of water uptake.

It can be observed from Figure 6 (a) that $d=30$ cm had the fastest responding of root water uptake to irrigation while $d=10$ cm had the slowest. Maximum water uptake values between irrigations for $d=30$ cm

were larger than those for $d=20$ and 10cm at the first 300 h. However, afterwards, the trend was opposite, with $d=10$ cm had the maximum absorption peak and $d=30$ cm had the minimum. The results of the other scenarios with different combinations of discharge flux and irrigation frequency were similar (data not shown). From Figure 6 (b), we noted that the fluctuations of root water uptake for $q=3 \text{ L}\cdot\text{h}^{-1}$ were slightly larger than that for $q=2 \text{ L}\cdot\text{h}^{-1}$, while the smallest fluctuation occurred for $q=1 \text{ L}\cdot\text{h}^{-1}$. Similar trends were also obtained for the other scenarios with various irrigation frequency and lateral depth (data not shown). Furthermore, when investigated the effect of irrigation frequency on water uptake, we observed that continuous application of water could led to larger root water uptake fluctuations between irrigations (data not shown).

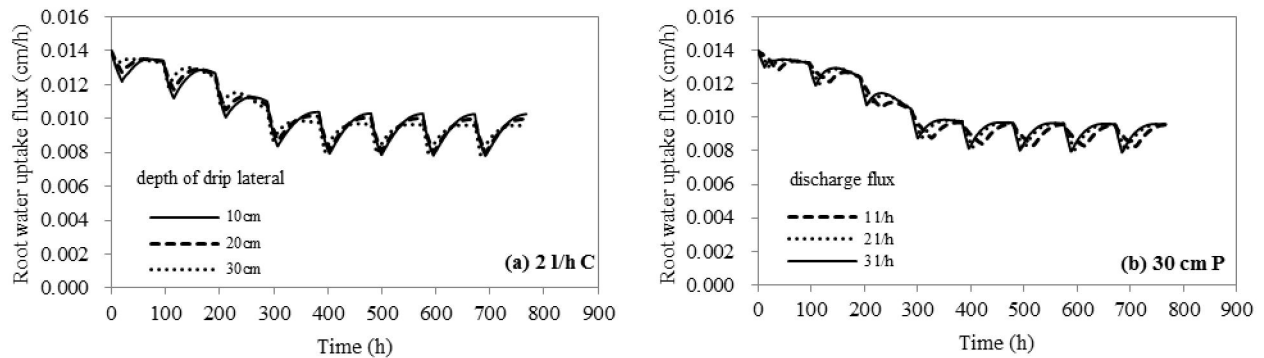


Figure 6 Water uptake fluxes by roots for (a) different lateral depth (scenarios 2c10, 2c20, 2c30,) and (b) different discharge rate (Scenarios 1P30, 2P30, 3P30).

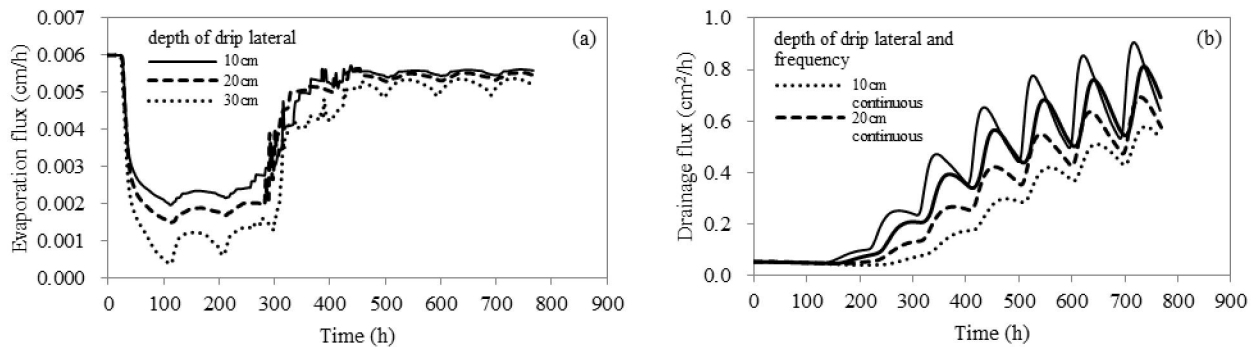


Figure 7. Fluxes of (a) evaporation for different lateral depth (Scenarios 1C10, 1C20, 1C30) and (b) drainage for different combinations of lateral depth and irrigation frequency (Scenarios 1C10, 1C20, 1C30, 1P30). Discharge rate was 1 L/h.

Figure 7 demonstrated the effect of lateral depth on the soil evaporation for continuous irrigation (Table 3.3, scenario 1C₁₀, 1C₂₀, 1C₃₀). The water flux at the domain surface exhibited a roughly cyclic behavior caused by the periodic irrigations, with flux values

increasing as the installation decreased. A trend of tempestuously declining occurred for the first 100 h and little trend was found for 100-300 h, but thereafter, the evaporation flux augmented acutely during 300-450 h and then tended to stable change. This variation may

be because that, during the first 100 h, the water content in the top soil declined rapidly due to high root water uptake (as shown in Figure 6), thereby resulting in the fast decrease of evaporation. However, with the process of irrigation, the wetted soil surface increased and fluctuated with time, which led to the variation trend during 100-768 h. In addition, regardless of the lateral depth, we noted that the evaporation rate values did not change obviously as the discharge rate increased (data not shown). A similar cyclic water flux behavior was also obtained for the pulsed irrigation (data not shown) although the water flux values were slightly higher than that for the continuous irrigation.

The influence of lateral depth on the drainage boundary flux for continuous irrigation (Table 3.3, scenario 1C₁₀, 1C₂₀, 1C₃₀) was shown in Figure 7. The water flux at the domain bottom (i.e. leaching) showed a strong cyclic effect between irrigations, and the flux values increased with the lateral depth, indicating under deep lateral installation a lot of water will not be utilized by tree. Besides, it can also be observed that the drainage flux kept stable during the first 150 h, but thereafter, it increased rapidly with shallower installation having much smaller fluctuations and minimum drainage flux values between irrigations. As expected, when the irrigation frequency changed to pulsed (Table 3.3, scenario 1C₃₀, 1P₃₀), we noted that the fluctuations and maximum values of water flux

between irrigations reduced (Figure 7) due to more upward and lateral water infiltration (Figure 4), whereas the degree of reduction decreased as the emitter flux increased (data not shown). This may also explain why more water was retained in the 0-30 cm soil layer under pulsed irrigation than that in continuous irrigation (Figure 55). Similar trends were also obtained for the other scenarios with various discharge rates. In addition, for a given lateral depth and irrigation frequency, we noted the increase of discharge rate had no regular effect on the drainage flux (data not shown).

3.2.2 The optimal irrigation strategy

Cumulative amounts of applied water, root water uptake, soil evaporation, and deep leaching were presented in Table 4. The cumulative soil evaporation varied greatly with the lateral depth, but was only little affected by the dripper flux and irrigation frequency, which was consistent with the observed impacts of lateral depth, discharge rate, and irrigation frequency on evaporation flux (Figure). Furthermore, it can be clearly observed that both increase in installation and continuous water application can significantly enhance the amount of deep leaching. However, the changes in emitter flow did not cause regular effects on leakage, except that in continuous irrigation $q=2 \text{ L}\cdot\text{h}^{-1}$ had the maximum drainage while in pulsed irrigation $q=1 \text{ L}\cdot\text{h}^{-1}$ had the minimum.

Table 4. Amount of applied water, root uptake, evaporation, drainage, and irrigation frequency for different combinations of discharge rate, lateral depth, and irrigation frequency.

| Scenario code | Discharge rate (L/h ⁻¹) | Applied water (cm ²) | Root uptake (cm ²) | Evaporation (cm ²) | Drainage (cm ²) | Irrigation frequency (%) |
|---|-------------------------------------|----------------------------------|--------------------------------|--------------------------------|-----------------------------|--------------------------|
| Drip lateral depth=10 cm, Continuous irrigation | | | | | | |
| 1C ₁₀ | 1 | 1534 | 802.11 | 334.28 | 170.18 | 52.3% |
| 2C ₁₀ | 2 | 1534 | 809.61 | 330.39 | 187.33 | 52.8% |
| 3C ₁₀ | 3 | 1534 | 814.11 | 331.93 | 179.14 | 53.1% |
| Drip lateral depth=20 cm, Continuous irrigation | | | | | | |
| 1C ₂₀ | 1 | 1534 | 805.23 | 320.56 | 221.56 | 52.5% |
| 2C ₂₀ | 2 | 1534 | 811.58 | 316.95 | 235.54 | 52.9% |
| 3C ₂₀ | 3 | 1534 | 815.41 | 320.87 | 222.15 | 53.2% |
| Drip lateral depth=30 cm, Continuous irrigation | | | | | | |
| 1C ₃₀ | 1 | 1534 | 796.74 | 278.19 | 309.91 | 51.9% |
| 2C ₃₀ | 2 | 1534 | 805.22 | 281.13 | 315.01 | 52.5% |
| 3C ₃₀ | 3 | 1534 | 808.82 | 286.89 | 288.58 | 52.7% |
| Drip lateral depth=10 cm, Pulsed irrigation | | | | | | |
| 1P ₁₀ | 1 | 1534 | 786.46 | 334.11 | 148.51 | 51.3% |
| 2P ₁₀ | 2 | 1534 | 801.96 | 332.41 | 164.84 | 52.3% |
| 3P ₁₀ | 3 | 1534 | 807.31 | 331.89 | 171.93 | 52.6% |
| Drip lateral depth=20 cm, Pulsed irrigation | | | | | | |
| 1P ₂₀ | 1 | 1534 | 795.79 | 321.87 | 192.39 | 51.9% |
| 2P ₂₀ | 2 | 1534 | 805.1 | 320.04 | 214.06 | 52.5% |
| 3P ₂₀ | 3 | 1534 | 809.82 | 320.69 | 216.14 | 52.8% |
| Drip lateral depth=30 cm, Pulsed irrigation | | | | | | |
| 1P ₃₀ | 1 | 1534 | 792.19 | 280.94 | 271.4 | 51.6% |

| | | | | | | |
|------------------|---|------|--------|--------|--------|-------|
| 2P ₃₀ | 2 | 1534 | 799.05 | 280.59 | 288.57 | 52.1% |
| 3P ₃₀ | 3 | 1534 | 803.09 | 284.41 | 283.24 | 52.4% |

Cumulative seasonal root water uptake values ranged from 802.11 to 814.11 cm² as discharge rate increased from 1 to 3 l·h⁻¹ for the continuous irrigation scenario ($d=10$ cm) and from 786.46 to 807.31 cm² for the pulsed irrigation scenario ($d=10$ cm), although the root water uptake were generally higher for continuous irrigation scenarios. As the lateral depth increased, maximum root water uptake always occurred in the 20 cm lateral depth scenarios. Due to the spatially varying soil moisture wetting around subsurface laterals, the irrigation efficiency (IE) can be defined as the ratio of the cumulative root water uptake to the total applied water. Although the amount of applied water was equal to 100% EP_{pot}, the IEs of all the 18 irrigation scenarios were relative low, ranging just from 51.6 to 53.2 %. This may be attributed to that, in our numerical simulations, the water uptake compensation effect of *P. tomentosa* was neglected, and thereby led to the reduced water uptake from the drier part in the rhizosphere could not be balanced by increasing uptake

4. Conclusions

In this work, for the purpose of selecting the optimal irrigation management strategy for the *P. tomentosa* pulp plantation, we investigated the performance of 18 irrigation scenarios including different combinations of three discharge rates, a range of lateral depths, and various irrigation frequencies. Analyses were performed using numerical simulations performed with the HYDRUS (2D/3D) software package. The conclusions are as follows:

(1) The numerical simulations showed that the geometry of soil wetting patterns were greatly influence by the emitter flux, lateral installation depth, and water application frequency. Decrease in discharge rate but keeping the amount of applied water the same could increase the dimensions of the wetting volume by decreasing the water moisture gradient behind the wetting front. The lateral depth can influence both the shapes and dimensions of the wetting patterns, and as the lateral depth increased, the radius and depth of the wetting volume increased accordingly. Pulsed irrigation led to slight increase in the dimensions of the wetted volume but again at lower water content gradient.

(2) In all the irrigation scenarios, the final water storages in 30-100 cm had no obvious difference, but in 0-30 cm we found that both pulsed irrigation and shallower lateral depth could result in more water being retained.

(4) From the perspective of increasing irrigation efficiency and reducing the negative effects on the environment, the combination of 3 L·h⁻¹ discharge rate, 10 cm lateral depth, and continuous irrigation is the optimal subsurface drip irrigation management strategy

in the less-stressed region in the rooting zone such as the SDI wetting volume. In fact, there is a strong water uptake compensation mechanism in poplar trees (**Error! Reference source not found.**; **Error! Reference source not found.** *et al.* 1999), so ignoring the root water uptake compensatory effect will inevitably lead to the research results deviate from the reality. Nevertheless, we believe that will not significantly affect us to select the optimal irrigation strategies in this study. From Table 44, we found that scenario 3C₁₀ and 3C₂₀ had the relative high irrigation efficiency, which were 53.1 and 53.2% respectively. However, when taking the effect of irrigation on environment and active root zone water storage into account, scenario 3C₁₀ is the better irrigation strategy, because scenario 3C₂₀ had higher summation of soil evaporation and deep leakage (Table 44)while 3C₁₀ had more water retained in the active root zone (0-30 cm) (Figure 5).

in our *P. tomentosa* plantation. However, our conclusion was derived by neglecting the root water uptake compensation effect, and if we took it into account the final result may be somewhat different.

Acknowledgements

This research was jointly supported by the Special Fund for National Forestry Scientific Research in the Public Interest (201004004), the Open Fund of the Beijing Forestry University '985' Advantage Subject Innovation Platform for Research on High Quality and Efficient Silviculture and Management techniques (000-1108003), and Strategic Scientific Project foundation of Eleventh Five-Year Plan for the research on carbon sequestration techniques and demonstration of fast-growing and high-yield plantations in Northern China (2008BAD95B07-01).

Corresponding Author:

Liming Jia
Key Laboratory for Silviculture and Conservation of
Ministry of Education
Beijing Forestry University
Beijing 100083, China
E-mail: jjalm2011@yahoo.com.cn

References

1. China Paper Association. The annual report of China's paper industry in 2008. China Pulp & Paper Industry 2009; (5): 6-17.
2. He XY. China's pulp and paper mills need to focus more on their fiber strategy-How to secure the future fiber supply?. China Pulp & Paper Industry 2008;

- 29(15): 20-23.
3. Li JH, Song HZ, Xue YC, Zhang QW, Li SG Present situations and development strategy on raw material of wood fiber for pulp and paper industry in China. *World Forestry Research* 2003; (6): 32-35.
 4. Zhu ZT, Kang XY, Zhang ZY. Studies on selection of natural triploid of *populous tomentosa*. *Scientia Silvae Sinicae* 1998; 34(4): 22-31.
 5. Laureysens I, Bogaert J, Blust R, Ceulemans R. Biomass production of 17 poplar clones in a short-rotation coppice culture on a waste disposal site and its relation to soil characteristics. *Forest Ecology and Management* 2004; 187(2-3): 295-309.
 6. Spinelli R, Hartsough BR. Harvesting SRF poplar for pulpwood: Experience in the Pacific Northwest. *Biomass and Bioenergy* 2006; 30(5): 439-445.
 7. Dillen SY, Marron N, Bastien C, Ricciotti L, Salani F, Sabatti M, Pinel MPC, Rae AM, Taylor G, Ceulemans R. Effects of environment and progeny on biomass estimations of five hybrid poplar families grown at three contrasting sites across Europe. *Forest Ecology and Management* 2007; 252(1-3):12-23.
 8. Shock CC, Feibert EBG, Seddigg M, Saunders LD. Water requirements and growth of irrigated hybrid poplar in a semi-arid environment in eastern Oregon. *Western Journal of Applied Forestry* 2002; 17(1): 46-53.
 9. Coyle DR, Coleman MD. Forest production responses to irrigation and fertilization are not explained by shifts in allocation. *Forest Ecology Management* 2005; 208(1-3): 137-152.
 10. Jia LM, Xing CS, Li JR, Wei YK. Productivity and benefit analysis of fast-growing and high-yield plantations of poplar under subsurface drip irrigation. *Journal of Beijing Forestry University* 2005; 27(6): 43-49.
 11. Wang W, Li GY, Duan ZS, Sun XZ. Experimental study on modifying wetting patterns of subsurface drip irrigation through engineering measures. *Water Saving Irrigation* 2000; 3: 22-24.
 12. Wang BF, Yang XH, Jiang ZP, Hao YG, Zhang JB. The responses of soil properties and tree's growth to irrigation in poplar timber woodland of arid region. *Journal of Arid Land Resources and Environment* 2006; 20 (6): 156-162.
 13. Vörösmarty CJ, Green P, Salisbury J, Lammers RB. Global water resources: vulnerability from climate change and population growth. *Science* 2000; 289(5477): 284-288.
 14. Fillion M, Brisson J, Teodorescu TI, Sauve S, Labrecque M. Performance of *Salic viminalis* and *Populus nigra* × *Populus maximowiczii* in short rotation intensive culture under high irrigation. *Biomass and Bioenergy* 2009; 33(9): 1271-1277.
 15. Shi XN, Zhang ZW, Huang ZQ. Application of drip irrigation in sandy land shelterbelt. *Forest Research* 2004; 17(S): 15-22.
 16. Jia LM, Wei YK, Li YA, Yang L, Xing CH. The growth and photosynthesis of poplar trees in fast-growing and high-yield plantations with subterranean drip irrigation. *Scientia Silvae Sinicae* 2004; 40(2): 61-67.
 17. Wei YK, Jia LM, Wang L, Qiu GQ, Xing CS. Characteristics of root growth in a fast-growing and high-yield poplar plantation. *Frontiers of Forestry in China* 2008; 3 (1): 98-105.
 18. Wei YK. A study on the fast-growing and high-yield mechanism of poplar plantations and the irrigation system on subsurface drip irrigation on sandy soil. Msc Thesis, Beijing Forestry University, Beijing, 2003.
 19. Su NH, Midmore DJ. Two-phase flow of water and air during aerated subsurface drip irrigation. *Journal of Hydrology* 2005; 313(3-4): 158-165.
 20. Ju XT, Xing GX, Chen XP, Zhang SL, Zhang LJ, Liu XJ, Cui ZL, Yin B, Christie P, Zhu ZL, Zhang FS. Reducing environmental risk by improving N management in intensive Chinese agricultural systems. *Proceedings of the National Academy of Sciences of the United States of America*. 2009; 106(9), 3041-3046.
 21. Cook FJ, Thorburn PJ, Fitch P, Bristow KL. WetUp: a soft tool to display approximate wetting patterns from drippers. *Irrigation Science* 2003; 22(3-4): 129-134.
 22. Singh D K, Rajput TBS, Singh DK, Sikarwar HS, Sahoo RN, Ahmad T. Simulation of soil wetting pattern with subsurface drip irrigation from line source. *Agricultural Water Management* 2006; 83(1-2): 130-134.
 23. Elmaloglou S, Diamantopoulos E. Simulation of soil water dynamics under subsurface drip irrigation from line sources. *Agricultural Water Management* 2009; 96(11): 1587-1595.
 24. Cote CM, Bristow BL, Charlesworth PB, Cook FJ, Thorburn PJ. Analysis of soil wetting and solute transport in subsurface trickle irrigation. *Irrigation Science* 2003; 22(3-4): 143-156.
 25. Skaggs TH, Trout TJ, Simunek J, Shouse PJ. Comparison of HYDRUS-2D simulations of drip irrigation with experimental observations. *Journal of irrigation and drainage engineering* 2004; 130(4): 304-310.
 26. Gardenas AI, Hopmans JW, Hanson BR, Simunek J. Two-dimensional modeling of nitrate leaching for various fertigation scenarios under microirrigation. *Agricultural Water Management* 2005; 74(3): 219-242.
 27. Siyal AA, Skaggs TH. Measured and simulated soil wetting patterns under porous clay pipe sub-surface irrigation. *Agricultural Water Management* 2009; 96(6): 893-904.
 28. Block RMA, van Rees KCJ, Knight JD. A review of fine roots dynamics in *Populus* plantations. *Agroforestry Systems* 2006; 67(1): 73-84.
 29. Simunek J, Sejna M, van Genuchten MTh. The HYDRUS software package for simulating two- and

- three-dimensional movement of water, heat, and multiple solutes in variably-saturated media. International Ground Water Modeling Center, Calif, 2006.
30. Van Genuchten MTh. A closed-form equation for predicting the hydraulic conductivity of unsaturated soils. *Soil Science of America Journal* 1980; 44(5): 892-898.
 31. Schaap MG, Leig FJ, van Genuchten MTh. Rosetta: a computer program for estimating soil hydraulic properties with hierarchical pedotransfer functions. *Journal of Hydrology* 2001; 251(3-4): 163-176.
 32. Xie XQ, Wang LJ. Monitoring of water environmental factors. China Standard Press, Beijing, 1998.
 33. Feddes RA, Kowalik PJ, Zaradny H. Simulation of field water use and crop yield. John Wiley and Sons, New York, 1978.
 34. Shock CC, Flock R, Feibert E, Shock CA, Pereira A, Jensen L. Irrigation monitoring using soil water tension. Oregon State Univ. Ext. Serv. EM 8900, 2005.
 35. Boast CW, Robertso, TM. A 'micro-lysimeter' method for determining evaporation from bare soil: description and laboratory evaluation. *Soil Science Society of America Journal* 1982; 46(4): 689-696.
 36. Smith DS, Wellington AB, Nachlinger JL, Fox CA. Functional response of riparian vegetation to stream flow diversion in the eastern Sierra Nevada. *Ecological Applications* 1991; 1(1): 89-97.
 37. Zhang HP, Morison JIL, Simmonds LP. Transpiration and water relations of poplar trees growing to the water table. *Tree Physiology* 1999; 19(9): 563-573.

3/30/2013